Duality and phase diagram of one-dimensional transport

2007 J. Phys. A: Math. Theor. 40 1703

(http://iopscience.iop.org/1751-8121/40/8/001)

IOP PUBLISHING JOURNAL OF PHYSICS A: MATHEMATICAL AND THEORETICAL

J. Phys. A: Math. Theor. **40** (2007) 1703–1710 doi:10.1088/1751-8113/40/8/001

Duality and phase diagram of one-dimensional transport

Somendra M Bhattacharjee

Institute of Physics, Bhubaneswar 751 005, India
and
Saha Institute of Nuclear Physics, Kolkata 700 064, India

E-mail: somen@iopb.res.in

Received 6 November 2006, in final form 13 January 2007
Published 6 February 2007
Online at stacks.iop.org/JPhysA/40/1703

Abstract
The idea of duality in one-dimensional nonequilibrium transport is introduced by generalizing the observations by Mukherji and Mishra. A general approach is developed for the classification and characterization of the steady state phase diagrams which are shown to be determined by the nature of the zeros of a set of coarse-grained functions that encode the microscopic dynamics. A new class of nonequilibrium multicritical points has been identified.

PACS numbers: 05.40.−a, 02.50.Ey, 64.60.−i, 89.75.−k

1. Introduction

Models involving the transport of particles from one end to the other along a one-dimensional track obeying some form of mutual exclusion are typical nonequilibrium problems which have found current relevance among others in molecular motors carrying cargo on a track in biological systems [1]. These models are important because of the different types of steady state phases and the possibility of nonequilibrium phase transitions even in one dimension [2–9], especially under open boundary conditions. The fact that the boundary conditions determine the phase transitions and the intimate connection between bulk and boundary transitions [2, 3] make these nonequilibrium problems different from equilibrium ones.

1.1. Phases and response functions

As an example, consider the asymmetric exclusion process (ASEP) on a one-dimensional lattice of $N(\to\infty)$ sites. Particles are injected at site $i = 1$ at a rate α (i.e probability that a particle is injected in a short time interval $\mathrm{d}t$ is $\alpha\,\mathrm{d}t$) and withdrawn at site $i = N$ at a rate $1 - \gamma$. The particles hop on the lattice as per preassigned rules, like hopping to the next site if it is empty [4, 5], or hopping rates depending on interactions among the particles on the

track, etc [6, 7]. In addition, there may be non-conserving processes, allowing addition to or deletion from the track [8], or correlated evaporation-deposition [1, 9].

For a coarse-grained description, one uses the local density $\rho(x,t)$ in continuum ($x \in [0,1]$ by a rescaling of the total length). The sensitivity to the boundary rates can be measured by the response functions

$$\chi_\mu \equiv \frac{\partial M}{\partial \mu}, \quad \text{where} \quad \mu = \alpha \text{ or } \gamma \quad \text{and} \quad M = \int_0^1 \mathrm{d}x\, \rho(x) \tag{1}$$

is the steady state spatially averaged density. The steady state phases are distinguished by the density profile $\rho(x)$ and the response functions. The phases are represented in phase diagrams in the space of the externally imposed rates α, γ at the two boundaries. Any two points in the α–γ space are said to be in the same phase if they can be connected by a continuous path along which the density profile or the response functions change smoothly. The phases observed are generally of the following types. (i) Injection (withdrawal) rate dominated, to be called the α-phase (γ-phase). In the α-phase, $\chi_\alpha \sim O(1)$ but $\chi_\gamma = 0$, while in the γ-phase, it is the other way round. (ii) A shock phase consisting of piecewise continuous densities, with both $\chi_{\alpha,\gamma} \neq 0$. (iii) special phases, e.g., a phase with maximum possible current through the system ($\chi_{\alpha,\gamma} \approx 0$), or both $\alpha-$ and $\gamma-$ phases present [9]. The phases are separated by first-order or continuous transitions, and special critical points have also been observed. For the model of reference [8], it was shown that the bulk phase boundary for the shock phase is associated with a shockening transition, a depinning of a confined boundary layer from the end point [2]. More recently, for the same model, Mukherji and Mishra identified a companion of the shockening transition in the form of a boundary transition inside a bulk phase [3].

The purpose of this paper is to identify the relevant features of the dynamic rules which determine the generic nature of the nonequilibrium phase diagram. We introduce in a model independent way the idea of duality between the shock phase boundary or the shockening transition and a boundary transition, generalizing the results of reference [3]. From this, the existence of a critical point can be inferred and the nature of the nonequilibrium phase diagrams can be obtained. This approach predicts a new class of nonequilibrium multicritical points.

2. Dynamics and steady states: definitions of S_i s

In a continuum limit for large N (with lattice spacing $a \ll L = Na$), the time variation of $\rho(x,t)$ can be written in the form of a continuity equation as

$$\frac{\partial \rho(x)}{\partial t} + \frac{\partial J_0(x,t)}{\partial x} = S_0(\rho, t), \tag{2}$$

where the right-hand side is the explicit non-conserving contribution and $J_0(x,t)$ is the current at the site. In a mean field approximation, the current is taken to be an implicit function of position and time through the density, so that J_0 can be split into two parts, namely a bulk contribution $J(\rho)$ and a Fick's law-type current determined by the density gradient

$$J_0 = -\epsilon S_2(\rho)\frac{\partial \rho}{\partial x} + J(\rho(x,t)). \tag{3}$$

The steady state density profile then satisfies

$$-\epsilon \frac{\mathrm{d}}{\mathrm{d}x} S_2(\rho)\frac{\mathrm{d}\rho}{\mathrm{d}x} + S_1(\rho)\frac{\mathrm{d}\rho}{\mathrm{d}x} + S_0(\rho) = 0, \tag{4}$$

with $S_1(\rho) = \mathrm{d}J(\rho)/\mathrm{d}\rho$, and the boundary conditions $\rho(0) = \alpha$ and $\rho(1) = \gamma$. A form such as equation (3) for $J_0(\rho)$ has been shown by Chakrabarti [10] to arise naturally in a renormalization group-type approach for transport processes and failures of fibre bundles.

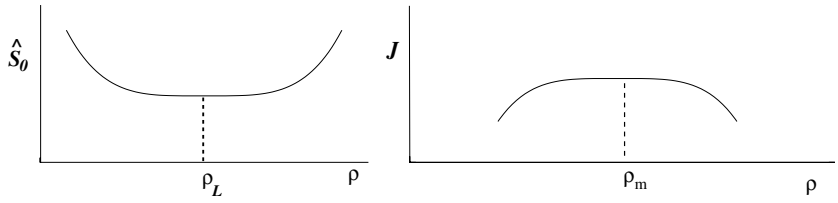

Figure 1. Schematic diagram for $\hat{S}_0(\rho)$ and $J(\rho)$ showing ρ_L and ρ_m.

The microscopic dynamic rules determine the functions $S_0(\rho)$, $S_2(\rho)$, $J(\rho)$, $S_1(\rho)$. Various approximations for $J(\rho)$ are in use; if known, one may use a current that includes the correlations in some way [6], or otherwise one may use a direct continuum limit of the rules. For example, for ASEP, $J_0 = \rho_{i-1}(1-\rho_i) - \rho_i(1-\rho_{i+1})$ (i being the site index) leads to the above form in the continuum limit with $\epsilon = a/2N$ and $S_2(\rho) = 1$. For boundary driven transitions, the smallness of ϵ is essential, and we see that this smallness is controlled by the parameter a/N. Equation (4) reduces to a first-order equation for $\epsilon \to 0$, but then it cannot in general satisfy the two boundary conditions. There lies the importance of the ϵ term, no matter how small, even though it looks innocuous in the bulk limit. A new scale $\tilde{x} = x/\epsilon$ appears in the problem. For example, the discontinuity at a shock will be rounded on a scale of $\tilde{x}$ but would look sharp on a bigger scale.

2.1. Nature of S_0

There are two special densities coming from $S_{0,1}(\rho)$ as the characteristics of the dynamics (figure 1). Let us first consider $S_0(\rho)$. The non-conserving dynamics by itself is given by $\mathrm{d}\rho/\mathrm{d}t = S_0(\rho) \equiv -\mathrm{d}\hat{S}_0/\mathrm{d}\rho$. This shows that the system would evolve to a time-independent density ρ_L for which $S_0(\rho_L) = 0$, or, equivalently, the free energy like function $\hat{S}_0(\rho)$ is an extrema. For the stability of the $\rho = \rho_L$ state, $\hat{S}_0(\rho)$ should be a minimum (figure 1), and therefore a simple choice would be

$$\hat{S}_0(\rho) \approx \Omega(\rho - \rho_L)^{2q}, \qquad (q \geqslant 1). \tag{5}$$

The most commonly studied case corresponds to Langmuir kinetics [8] which is $q = 1$ in equation (5) with Ω as the net flux of incoming particles. The conserved case (no evaporation/deposition) of equation (4) is recovered in the limit $\Omega \to 0$. Instead of single-particle Langmuir kinetics, correlated evaporation–deposition cases may be considered where the track is in contact with an equilibrium interacting lattice gas at its multicritical point, for which the Landau free energy [11] would have $q \geqslant 2$.

2.2. Nature of S_1

Coming to $S_1(\rho)$, one notes that since the current is necessarily zero for both $\rho = 1$ (complete filling) and $\rho = 0$ (empty track), there has to be at least one maximum of $J(\rho)$. This then defines a special density ρ_m at which the current is maximum (figure 1). Since $S_1(\rho_m) = 0$, equation (4) shows that a discontinuity in the density is allowed at this density. Consequently, if there is a shock (a discontinuity in density in the $\epsilon \to 0$ limit), then it has to be centred around $\rho = \rho_m$. A general choice of J is

$$J(\rho) \approx J_{\mathrm{m}} - c(\rho - \rho_m)^{2p}, \qquad (c > 0,\ p \geqslant 1). \tag{6}$$

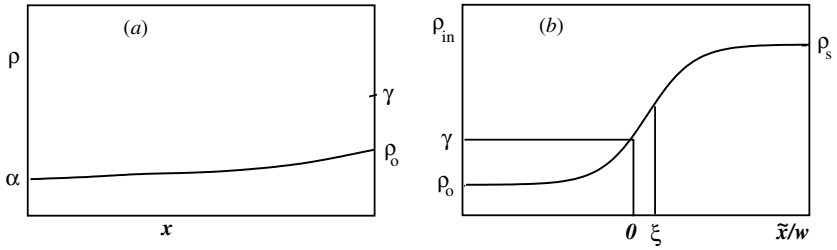

Figure 2. Schematic diagram of the outer and the inner or boundary layers. (*a*) Outer solution matches the boundary condition at $x = 0$ and gives $\rho = \rho_0$ at $x = 1$. The boundary condition at $x = 1$ requires $\rho = \gamma$. (*b*) Inner solution $\mathcal{I}(\tilde{x}/w + \xi)$ extrapolating ρ_o to γ. ρ_s is the other saturation value. The centre of the layer is at ξ. In the figure, it is outside the physical domain and so it is to be called a 'virtual origin'.

The two characteristic densities are independent of each other. However, $\rho_L = \rho_m$ is a very special case because the non-conserving processes try to maintain a density at which the conserved processes can accommodate a maximum current. The qualitative features and the exponents obtained here would remain the same for any $S_2(\rho) > 0$. Consequently, we consider the case with $S_2(\rho) = 1$. Special situations arise if $S_2(\rho)$ changes the sign. There can be cases with more than one zero of $S_0(\rho)$ as, e.g., in [9] with metastable states, and there could be cases with nonanalytic [7], or multipeaked [6] $J(\rho)$. Such cases will be discussed elsewhere.

3. Boundary layer analysis: outer and inner densities

To handle the two scales in equation (4), a boundary layer approach is used. We summarize the procedure here and refer to [2, 3, 12] for details on the procedure. Consider the case where the density profile $\rho_{\rm out}(x)$, from equation (4) with $\epsilon = 0$, matches the boundary condition $\rho(0) = \alpha$. But, then, $\rho_{\rm o} \equiv \rho_{\rm out}(1) \neq \gamma$ as shown in figure 2(*a*). A different density profile (figure 2(*b*)) $\rho_{\rm in}(\tilde{x})$, where $\tilde{x} = (x - x_s)/\epsilon$, $(x_s = 1)$ extrapolates within a thin 'inner' region from $\rho_{\rm in}(-\infty) = \rho_{\rm o}$ to $\rho_{\rm in}(0) = \gamma$. Three possible situations are shown schematically in figure 3. The inner region satisfies equation (3) with $J_0 = J(\rho_{\rm o})$. The physical reason for this is that the current $J_0 = J(\rho_{\rm o})$ entering from the bulk (outer) region remains conserved in the inner layer because the inner region, to first order in ϵ, is too thin for the non-conservation to matter. A shock is formed only if the inner solution fails to satisfy the boundary condition. This happens if the inner solution saturates at the other end ($\rho_{\rm in}(\tilde{x}) \to \rho_{\rm s}$ as $\tilde{x} \to \infty$) [13]. If we define $S_1(\rho) = {\rm d}\hat{S}_1(\rho)/{\rm d}\rho$, then the matching condition and the saturation requirement for shock are ensured by two zeros of $\hat{S}_1(\rho)$, so that

$$\hat{S}_1(\rho) = -(\rho - \rho_{\rm o})(\rho - \rho_{\rm s})\Phi(\rho). \tag{7}$$

Note that $\rho_{\rm o} \leqslant \rho_m \leqslant \rho_{\rm s}$, and $\rho_{\rm o,s}$ depend on α.

The inner solution (figure 2(*b*)) is of the form $\mathcal{I}(\tilde{x}/w + \xi)$ with $\mathcal{I}(z) \to \rho_s$ or $\rho_{\rm o}$ as $z \to \pm\infty$. Here w is the width of the layer, and ξ gives the location of the centre of the layer. There are two types of densities [3], one bounded (B-type) between ρ_o and ρ_s, while the other one shows a divergence (U-type) with ${\rm d}\rho/{\rm d}x \sim -\rho^2$, or more generally, ${\rm d}\rho/{\rm d}x \sim -\rho^{2p}$. It is the B-type layers that lead to shock formation but not the U-type. A continuation of the density and the space beyond the range of [0, 1] is necessary. If the centre of the layer lies outside the physical domain, the origin is to be called a 'virtual origin'. This continuation

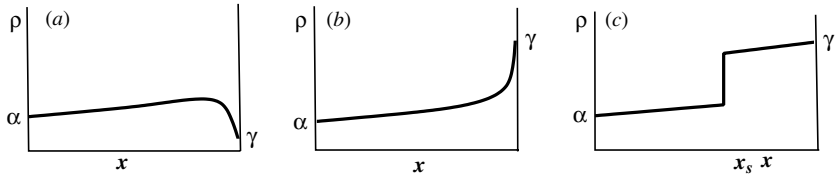

Figure 3. (*a*) A boundary layer at $x = 1$. This represents a depleted region at the end point. Part (*b*) shows an accumulated density at the right end. Part (*c*) shows a shock without any boundary layer at the end points. The inner layer connects the two outer solutions. This layer on the bulk scale looks like a discontinuity or a shock at $x = x_s$.

helps in getting the general form of the phase diagram. For a particular system, the real phase diagram may only be a small window around the point $\alpha = \gamma = \rho_m$ with the window size determined by the parameters of the problem, like Ω etc [8].

3.1. Shock and shockening transition

For a given α, as γ is changed, two different situations may arise. In one case, the origin or the centre of the layer shifts to $-\infty$ ($\xi \to -\infty$). In the other situation, the origin remains virtual and moves to infinity, $\xi \to +\infty$.

The first case is a thickening of the layer remaining pinned to the boundary. As $\xi \to -\infty$, the layer gets released from the boundary and moves into the bulk. The transition of a thin layer to a shock at $\gamma = \rho_s(\alpha)$ has been called a 'shockening' transition [2]. So long as the boundary layer stays pinned to the boundary, $\chi_\gamma \sim \epsilon\gamma/\hat{S}_1(\gamma) \to 0$ as $\epsilon \to 0$. In contrast, χ_α is nonzero. The phase, by definition, is then an α-phase. The bulk shock phase boundary is given by $\gamma = \rho_s(\alpha)$.

3.2. Duality and phase diagram

The occurrence of the two zeros of $\hat{S}_1(\rho)$ in equation (7) suggests that there has to be another line $\gamma = \rho_o(\alpha)$ at which $\xi \to +\infty$. We call this the Mukherji–Mishra (MM) dual boundary line because a similar feature was observed in [3] though for a particular model. As one crosses this MM line the boundary region goes from an accumulated (figure 3(*b*)) to a depleted (figure 3(*a*)) region, thereby separating the shockening (B-type) to nonshockening (U-type) boundary layers. This MM dual line is purely a boundary transition line, and its existence is a requirement for shock formation at $\gamma = \rho_s(\alpha)$. Since (ρ_o, ρ_s) need to occur in pair, we call the $\gamma = \rho_s(\alpha)$ as the dual line of the bulk phase boundary.

Once we know the bulk phase boundary and the dual line, we can obtain the width of the layer. From the asymptotic approach to the limits ρ_X, ($X = o$ or s), one gets from equation (7) $w^{-1} = (\rho_s - \rho_o)\Phi(\rho_X)$. This also shows the possibility of a critical point when w diverges. This happens if the shockening transition line and the dual line intersect. The intersection is at $\gamma = \rho_m$ and since $\rho_o \to \rho_s$, we find $w \to \infty$. For equation (6),

$$w \sim |\rho_o - \rho_s|^{-(2p-1)} \sim h^{-(2p-1)}, \tag{8}$$

where h is the height of the shock. The extra p-dependence comes from the fact that $\Phi(\rho) \to 0$ as $\rho \to \rho_m$ for $p > 1$. The bulk phase transition from the α-phase to the shock phase is of first order, because at the transition point the shock height is nonzero. On the other hand, the shock evolves from a zero height at the critical point so that it is a continuous transition. The line with a critical point is shown in figure 4(*a*). In case the two lines do not cross, there will

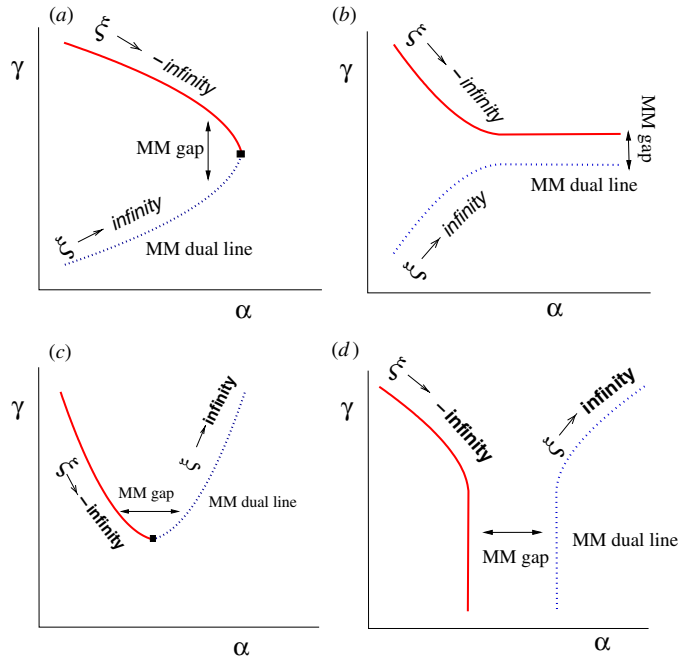

Figure 4. Possible phase boundaries (thick line) and dual lines (dotted). (*a*) and (*b*) for the α-phase with the shock forming at $x = 1$; (*c*) and (*d*) for the γ-phase with shock forming at $x = 0$. In (*a*) and (*c*) the intersection of the shock phase boundary and the MM dual line produces a critical point (filled square). No critical point in (*b*) and (*d*). The α, γ asymmetry depends on the relative values of ρ_L and ρ_m.

be no critical point and the lines will be symmetrically placed around $\gamma = \rho_m$. An example is shown in figure 4(*b*). So far, we have concentrated on the α-phase only. A similar analysis can be done for the γ-phase for which the shock is formed at $x = 0$. The inner solution is an increasing function of $\tilde{x}$ and so the shock is upward. Therefore, the shock formation now corresponds to $\xi \to -\infty$, while the dual line is for $\xi \to +\infty$. The two possible cases are shown in figures 4(*c*) and (*d*). In figure 4(*c*), there is a critical point at the intersection $\alpha = \rho_m$ of the two lines, while there is no critical point in figure 4(*d*).

Combining the two possibilities of the transitions (lines for $x = 1$ and for $x = 0$ of figure 4), we can now draw the global phase diagram. Combination of (*a*) and (*c*) of figure 4 gives the type known for $\rho_L = \rho_m$ ($K = 1$, the case of [2, 3, 8]) as in figures 5(*b*) and (*c*). Similarly, (*a*) with (*d*) of figure 4 gives figure 5(*d*), known for $\rho_L > \rho_m$, while (*b*) with (*c*) of figure 4 will be the case (figure 5(*e*)) for $\rho_L < \rho_m$. For $\gamma < \gamma_c = \rho_m$, on the α-phase side, the U-type boundary layer renders an effective boundary value ρ_m at $x = 1$, and therefore the critical behaviour continues for all γ [8, 3]. The shock on changing α evolves in height and shifts to $x = 0$. On the γ-phase side, the response function χ_γ undergoes a change on crossing the line $\gamma = \rho_m$, even though the bulk density distribution changes smoothly. The line $\gamma = \rho_m$ indicates a boundary transition, like the MM dual lines. In special situations it may also develop into a bulk phase boundary (e.g., $\rho_L \to \rho_m$, figure 5(*c*)). There is another possibility where the $x = 1$ and the $x = 0$ lines intersect thereby preempting the critical point, as in figure 5(*f*). Such a case is known in a special correlated nonconserved case of [9]. As mentioned earlier, a complete description of such a phase diagram would require more than one zero of $\hat{S}_0(\rho)$.

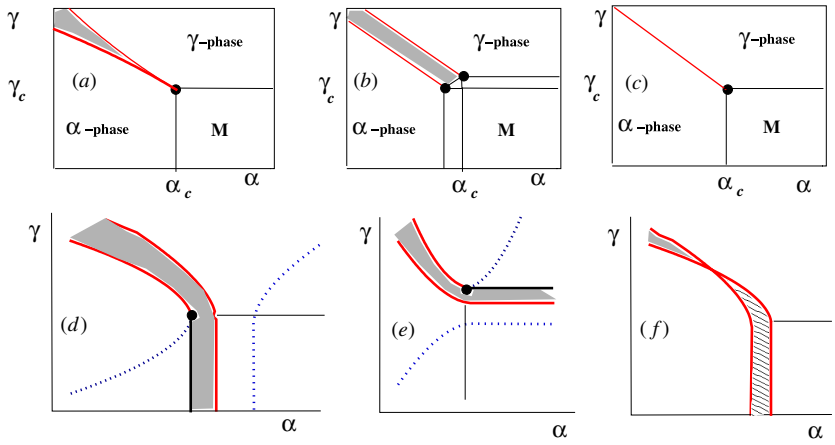

Figure 5. α–γ phase diagrams for (*a*), (*b*), (*c*) $\rho_L = \rho_m$, (*d*) $\rho_L > \rho_M$ and (*e*) $\rho_L < \rho_M$. The critical points are represented by filled circles. The shaded region is the shock region. In (*a*) $q > p$, (*b*) $q = p$ while (*c*) has no non-conserving part. The MM dual lines are shown in (*d*) and (*e*) only. (*f*) corresponds to a situation where the transition lines cross. Shock phase exists only in the top part.

The shape of the shockening curve near the critical point for $q = 1$ is given by $(\gamma - \gamma_c) \sim |\alpha - \alpha_c|^{1/2p}$. For $\gamma = \gamma_c = \rho_m$, the shock height vanishes on the shock side as $h \sim |\alpha - \alpha_c|^{\zeta'}$ with $\zeta' = 1/(2p+1)$. Though the $p = 1$ case is known in the literature, we find the exponents to depend on the nature of the current maximum (the value of p). These represent a class of multicritical points. For $\rho_L = \rho_m$, our analysis via the duality yields the nature of the critical points. For $q = p$, the phase boundaries are similar to the $q = p = 1$ case. However for $q > p$, the critical point is at $\alpha = \rho_m, \gamma = \rho_m$. We show a new type of phase diagram for a particular case with $\rho_m = 0.5$ in figure 5.

As one traverses the shock phase from one phase boundary to the other, say in figure 5(*b*), the shock position goes from $x = 1$ to $x = 0$. Now, if $\Omega \to 0$, the shock region collapses on to a line as in figure 5(*c*), which also means that the shock is uniformly distributed over the entire length. To get the density profile on this line in the phase diagram, one needs to average over the distribution of shocks[1]. This averaging yields the linear density profile one knows from exact solutions [4, 14][2]. In other words, even though the mean field theory puts a bias towards shock formation, a judicious use via the $\Omega \to 0$ limit yields correct results.

4. Conclusion

Based on the results obtained so far, we find that the topology of the phase diagram and critical points can be determined from the knowledge of a few coarse-grained features of the dynamics as determined by the zeros of the S-functions of equation (4). The duality helps in identifying the critical point and its description. Based on these results, we can enunciate the criteria to determine if changes in the microscopic rules of dynamics would affect the phase diagrams or the critical points. For the continuum description, if the perturbation of the rules changes only the densities ρ_L or ρ_m or both, without changing q and p, then the phase diagrams will

[1] I thank P K Mohanty for discussion on this point.

[2] This is consistent with the dynamic view at $\Omega = 0$ that the linear profile follows from a drift-less diffusive behaviour of the domain wall or shock, as discussed in [15]

be of similar type unless the special case of $\rho_L = \rho_m$ is reached or crossed. The exponents for the critical points on the phase diagram will change only if the perturbations modify the values of q and/or p.

In summary, we have introduced the idea of duality that can be stated as the MM theorem: 'Every shockening transition has a dual boundary transition and if the two lines (the shockening transition and the dual line) intersect, there is a critical point'. With the help of this duality, we can locate the critical point on the phase diagram and also its nature. The general approach allows us to establish a set of criteria to test if perturbations of rules are relevant for modifications of the phase diagram and critical points.

References

[1] Liggett T 1999 *Interacting Particle Systems: Contact, Voter and Exclusion Processes* (Berlin: Springer)
Stinchcombe R B 2002 *J. Phys.: Condens. Matter.* **14** 1473
[2] Mukherji S and Bhattacharjee S M 2005 *J. Phys. A: Math. Gen.* **38** L285
[3] Mukherji S and Mishra V 2006 *Phys. Rev.* E **74** 011116
[4] Derrida B *et al* 1993 *J. Phys. A: Math. Gen.* **26** 1493
Schütz G and Domany E 1993 *J. Stat. Phys.* **72** 277
[5] Evans M R *et al* 1995 *Phys. Rev. Lett.* **74** 208
Evans M R *et al* 1995 *J. Stat. Phys.* **80** 69
[6] Krug J 1991 *Phys. Rev. Lett.* **67** 1882
Hager J S *et al* 2001 *Phys. Rev.* E **63** 056110
Papkov V *et al* 2003 *Phys. Rev.* E **67** 066117
[7] Tripathy G and Barma M 1997 *Phys. Rev. Lett.* **78** 3039
Tripathy G and Barma M 1998 *Phys. Rev.* E **58** 1911
Harris R J and Stinchcombe R B 2004 *Phys. Rev.* E **70** 016108
[8] Parmeggiani A, Franosch T and Frey E 2003 *Phys. Rev. Lett.* **90** 086601
Parmeggiani A, Franosch T and Frey E 2004 *Phys. Rev.* E **70** 046101
Evans M R, Juhasz R and Santen L 2003 *Phys. Rev.* E **68** 026117
[9] Rakos A, Paessens M and Schuetz G M 2003 *Phys. Rev. Lett.* **91** 238302
[10] Chakrabarti B K 2006 *Physica* A **372** 162
[11] Huang K 1987 *Statistical Mechanics* (New York: Wiley)
[12] Nayfeh A H 1973 *Perturbation Methods* (New York: Wiley)
[13] Lighthill M J and Whitham G B 1955 *Proc. R. Soc.* A **229** 317
[14] Kolomeisky A B *et al* 1998 *J. Phys. A: Math. Gen.* **31** 6911